

## A MODIFIED FM SYNTHESIS APPROACH TO BANDLIMITED SIGNAL GENERATION

Joe Timoney, Victor Lazzarini and Tom Lysaght

Sound and Digital Music Technology Group,

NUI Maynooth,

Co. Kildare, Ireland

jtimoney@cs.nuim.ie

victor.lazzarini@nuim.ie

tlysaght@cs.nuim.ie

### ABSTRACT

Techniques for the generation of bandlimited signals for application to digital implementations of subtractive synthesis have been researched by a number of authors. This paper hopes to contribute to the variety of approaches by proposing a technique based on Frequency Modulation (FM) synthesis. This paper presents and explains the equations required for bandlimited pulse generation using modified FM synthesis. It then investigates the relationships between the modulation index and the quality of the reproduction in terms of authenticity and aliasing for a sawtooth wave. To determine the performance of this technique in comparison to others two sets of simulation results are offered: the first computes the relative power of the non-harmonic components, and the second uses the Perceptual Evaluation of Audio Quality (PEAQ) algorithm. It is shown that this technique compares well with the alternatives. The paper concludes with suggestions for the direction of future improvements to the method.

### 1. INTRODUCTION

The development of anti-aliasing oscillators for digital subtractive synthesis has attracted the interest of a number of researchers, and just recently a very comprehensive review paper was published that summarised the variety of approaches and also proposed significant optimisations to some of the techniques [1]. According to [1], the solutions to this problem can be classified into three groups:

1. Bandlimited algorithms that produce a fixed number of harmonics
2. Quasi-bandlimited algorithms that sample a low-pass filtered continuous time function
3. Algorithms based on spectral tilt modification

Most of the well-known algorithms belong to the second class of solutions, and have presented processing methods for Bandlimited Sinc Pulse trains [2] and Bandlimited step sequences [3] to produce the anti-aliasing oscillators. The key to both these techniques is the use of the Sinc function that is manipulated for the synthesis of both the bandlimited impulse and the bandlimited step function. Issues surrounding this approach have included ideal Sinc approximation errors, the need for additional control logic, and memory requirements [4]. This paper hopes to overcome some of these problems by proposing an alternative based on a modified FM synthesis approach for the generation of bandlimited pulses that can then be further pro-

cessed to produce the desired subtractive synthesis oscillator waveforms. The work was inspired by Moorer's classic paper [5] who examined the musical applicability of formulas directly descended from the original equations for FM synthesis. However, unlike the FM synthesis equations, their spectral description of the resulting waveforms contained Modified Bessel functions. This resulted in the partials of these spectra having amplitudes that change smoothly from one to the next without the unexpected appearance of insignificant partials that is characteristic of the original FM synthesis.

### 2. BANDLIMITED PULSE GENERATION

Following some manipulation of the formula for FM synthesis using Modified Bessel functions presented in [5], the equation for a bandlimited pulse can be written as

$$y(t) = e^{(k \cos(\omega t) - k)} \cos(\omega t) \quad (1)$$

where the Modulation index  $k$  and the frequency is  $\omega$ .

Figure 1 shows an example of such a bandlimited pulse. As can be seen from the Figure, Equation (1) will produce a train of smooth pulses at a frequency given by  $\omega$ .

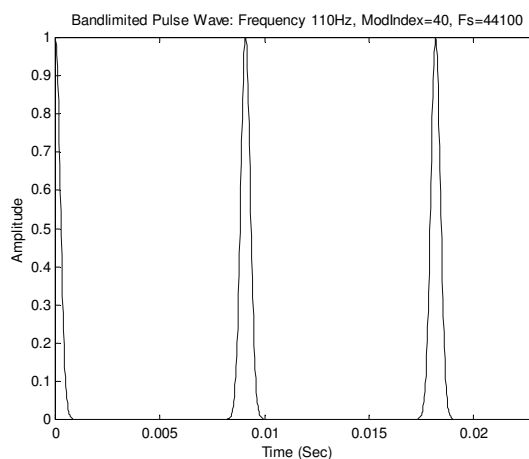


Figure 1: Example of a Bandlimited Pulse at a frequency of 110 Hz and a Modulation Index of 40.

The width, and therefore smoothness, of the pulse is determined by the modulating index  $k$  and lower values of  $k$  will give a broader pulse shape. This is illustrated in Figure 2 for the same pulse shown in Figure 1 with a modulation index of 10 (dashed line) and a modulation index of 40 (solid line). The pulse formed with the lower modulation index is wider.

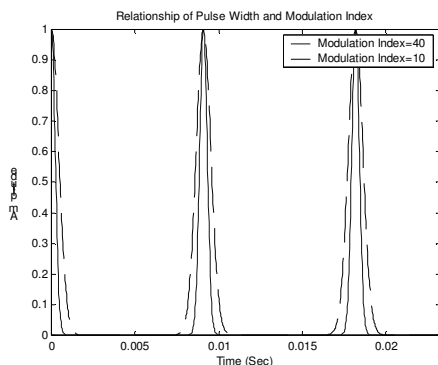


Figure 2: The Relationship between the Modulation Index and the width of the Pulse shown for a Modulation Index of 10 and a Modulation Index of 40.

The spectrum of the pulse train defined by Equation (1) is given by

$$X(\omega) = \frac{1}{e^k} \sum_{n=1}^{\infty} (I_{n-1}(k) + I_{n+1}(k)) \cos(n\omega) \quad (2)$$

where  $I_n(\cdot)$  is a modified Bessel function of the first kind of order  $n$ .

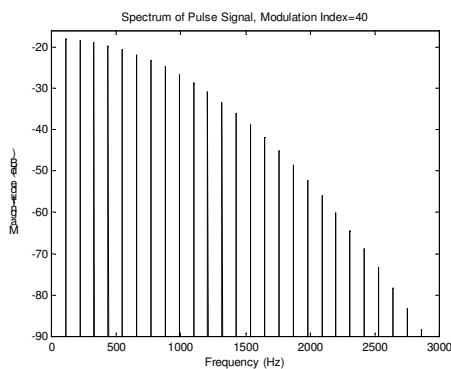


Figure 3: The harmonic magnitudes given by (2) for a 110 Hz pulse train generated with a Modulation Index of 40.

Examining Equation (2) it is clear that Equation (1) produces an harmonic spectrum whose harmonic amplitudes are determined by a sum of Modified Bessel functions and scaled by the factor  $1/e^k$ . This spectrum given by Equation (2) is plotted in Figure 3. From the plot it can be seen that the spectrum has a low-pass shape with the harmonic magnitudes demonstrating a smooth roll-off. This roll-off characteristic suggests that it should be possible to judiciously choose parameter values for the modulation index  $k$  in Equation (1) such that the pulse train waveform is effectively a bandlimited signal.

The rate of roll-off in the spectrum is determined by the modulation index  $k$ . To gain a deeper insight into the implications of Equation (2), it is worthwhile to investigate both the relationships between the amplitude of the modified Bessel function (scaled by  $1/e^k$ ) and the modulation index, and the order of modified Bessel function. Figure 4 shows a plot of the amplitudes of the scaled modified Bessel functions of orders 0 to 3 for modulation index values varying over the range 0 to 10. For the scaled modified Bessel Functions of order 0, its amplitude decreases with increasing modulation index. In contrast, for the others they increase firstly and then begin to decrease, with the point of change being later as the order increases in value. The behavior of these modified Bessel functions is different to the Bessel functions that appear in the more familiar FM synthesis equations that exhibit an oscillatory amplitude pattern with increasing modulation index [6]. Figure 4 suggests that for a spectrum determined by Modified Bessel functions by increasing or decreasing the modulation index the spectral harmonics will smoothly increase/decrease in magnitude giving a perceptual effect more reminiscent of an opening/closing lowpass filter.

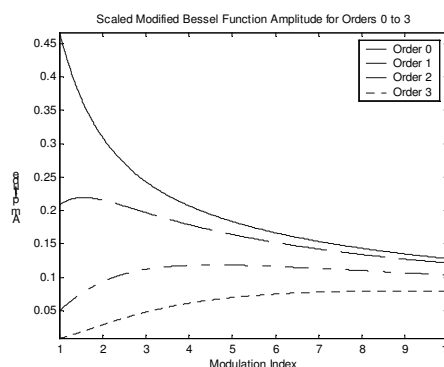


Figure 4: The Relationship between the Modulation Index and Amplitude of the Scaled Modified Bessel functions at orders 0, 1 and 2.

Also from Figure 4, it can be observed that the lower the order of the Modified Bessel function the greater its amplitude. This explains why the example spectrum in Figure 3 is lowpass in appearance, as the lower the frequency of an harmonic, the lower the order of the Modified Bessel function associated with its magnitude.

### 3. BANDLIMITED SAWTOOTH GENERATION

If a bandlimited pulse train is available it is possible to generate a bandlimited sawtooth wave by integration following the procedure given in [2]. The integration can be carried out using a filter whose  $z$ -transform is

$$H(z) = \frac{1}{1 - z^{-1}} \quad (3)$$

An important factor in the procedure is to remove the mean of the pulse train so that the sawtooth will be centred around a DC level of 0. For this pulse wave it was necessary to use a DC blocking filter [7] after the integration stage. The bandlimited

sawtooth generation system could thus be described by the block diagram in Figure 5.

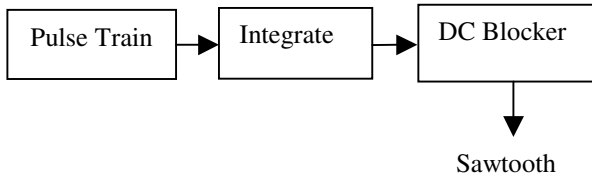


Figure 5: Sequence of operations to generate a bandlimited sawtooth from a bandlimited pulse train.

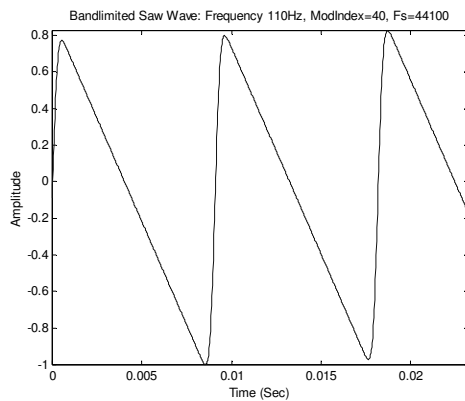


Figure 6: Bandlimited sawtooth created by applying the procedure shown in Figure 5 to the pulse train given in Figure 1

This procedure was applied to the pulse train given in Figure 1 and the sawtooth shown in Figure 6 resulted.

After demonstrating that a sawtooth can be generated using this method, a key question investigated here is what is the best value for modulation index  $k$  such that this bandlimited sawtooth most closely approximates an ideal digital sawtooth. It was demonstrated in the previous section that the higher the modulation index  $k$  the greater the magnitude of the higher frequency spectral harmonics. However, from Equation (2) it can be observed that the harmonics of the signal extend towards infinity. Therefore, a trade-off must be found that balances the magnitudes of the upper harmonics of the sawtooth against the magnitude of harmonics that will occur at greater than half the sampling frequency such that the aliasing distortion they cause is not perceptually significant. To measure this it is useful to have an expression for the harmonic magnitudes of the Bandlimited Sawtooth wave. This can be found by integrating Equation (2) with respect to frequency

$$X_{saw}(\omega) = \frac{e^{-k}}{(n\omega)} \sum_{n=1}^{\infty} (I_{n-1}(k) + I_{n+1}(k)) \sin(n\omega) \quad (4)$$

An experiment can then be made that will give the maximum value for the modulation index at any sawtooth frequency such that the harmonics that lie beyond half the sampling frequency are less than a defined threshold. Fortunately, because the magnitude of the harmonics exhibit a lowpass characteristic this meas-

urement can be constrained so that the threshold is applied to the magnitude of the first harmonic that appears after half the sampling frequency and can be determined using Equation (4). Choosing a threshold such that this harmonic is at least 90dB below the fundamental, the maximum modulation index with respect to a band of frequencies was determined and is plotted in Figure 7. In Figure 7 the x-axis displays frequency in terms of its respective midi-note value.

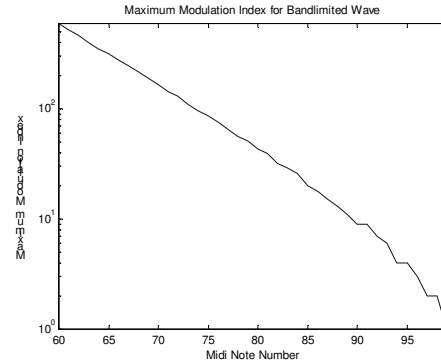


Figure 7: The maximum allowable modulation index shown with respect to midi-note value such that harmonics after half the sampling frequency are less than 90dB relative to the fundamental component.

The frequency points used in this analysis were obtained by finding the equivalent in Hertz ( $f_{Hz}$ ) of the midi note values 60 to 99, which are given by

$$f_{Hz} = 440 \times (2^{(midi\_note-69)/12}) \quad (5)$$

This set of midi-notes was chosen simply because many melodies lie within this note range. The maximum modulation index was found in an iterative manner. Using Equation (4), the dB difference between the magnitude of the fundamental component and the first harmonic after half the sampling frequency was evaluated for an increasing set of modulation index values commencing at zero and incrementing by one until the threshold of -90dB was exceeded.

It can be seen in Figure 7 that the maximum modulation index decreases from a value greater than 500 at midi note 60 down to approximately 1 at midi-note 99. The trend from low-to-high midi notes appears to be almost linear. Thus, in the upper octaves low values of modulation index are required to prevent aliasing distortion.

The next question addressed is how well does this bandlimited sawtooth, constrained to the maximum modulation index, approximate an ideal digital sawtooth created using additive sinewave synthesis techniques.

Figure 8 shows a plot that makes a comparison in dB between the summed harmonic magnitudes of the bandlimited sawtooth, computed using Equation (4), against those of the ideal digital sawtooth up to half the sampling frequency. At midi-note 60 the difference is just above 1.6dB. This difference increases in an approximately linear fashion to reach above 3.2dB at midi-note 99.

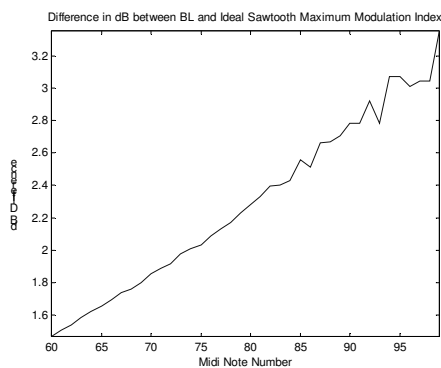


Figure 8: *dB difference between the modulation index constrained bandlimited sawtooth and the ideal digital sawtooth with respect to midi-note value.*

To get an impression of where in the spectrum the harmonic magnitudes of the bandlimited and ideal digital sawtooths begin to diverge, another experiment was carried out. It was designed to determine at which frequency the difference in harmonic magnitude between the two became  $-3\text{dB}$ . Figure 9 shows the result of this experiment.

In Figure 9 it is shown that at midi-note 60 the frequency at which the magnitudes differ is 5500 Hz. This suggests that it is in the vicinity of the 20<sup>th</sup> harmonic where the two spectra begin to diverge significantly. Up until midi-note 87, the frequency of spectral divergence does not change a lot. There is some oscillation around this value which is due to harmonic locations in each signal. After midi-note 87 up to midi-note 99 there is a strong oscillation between 5000 Hz and 7000Hz. However, this means that it is around the 4<sup>th</sup>, and then the 3<sup>rd</sup> harmonic where the two spectra diverge. Overall, as the pitch of the waveform increases the harmonic number at which the bandlimited sawtooth differs from the ideal digital sawtooth by 3dB or more increases.

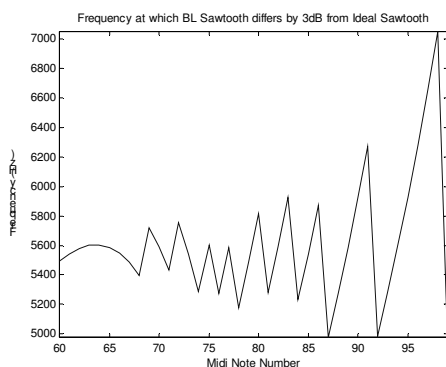


Figure 9: *Frequency at which the harmonic magnitudes of the bandlimited and the Ideal digital sawtooths begin to differ by  $-3\text{dB}$ .*

Considering Figures 7-9 together it appears that for lower pitched notes the maximum modulation index that keeps aliased components below 90dB in the bandlimited sawtooth is high and this decreases roughly linearly with increasing pitch. However, the lowering of the modulation index has the drawback

of increasing the spectral difference between the bandlimited sawtooth and the ideal digital sawtooth as the pitch increases.

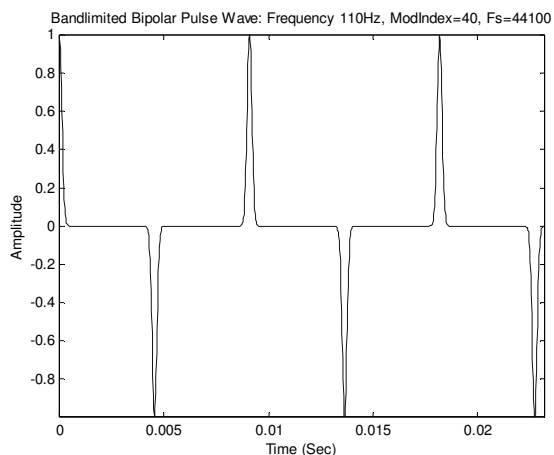


Figure 10: *Bipolar Bandlimited Pulse waveform.*

#### 4. GENERATING OTHER BANDLIMITED WAVEFORMS

Equation (1) can be modified by doubling the frequency of the cosine in the exponent

$$y(t) = e^{(k \cos(2\omega t) - k)} \cos(\omega t) \quad (6)$$

This will create a bipolar bandlimited pulse wave as shown in Figure 10. The parameters used to generate this wave were the same as those for Figure 1.

Integrating this waveform using the integrator defined in Equation (3) will then produce a Bandlimited Square wave, and by further integrating this square wave will produce a Bandlimited triangle waveform. An example of these is shown in Figures 11 and 12.

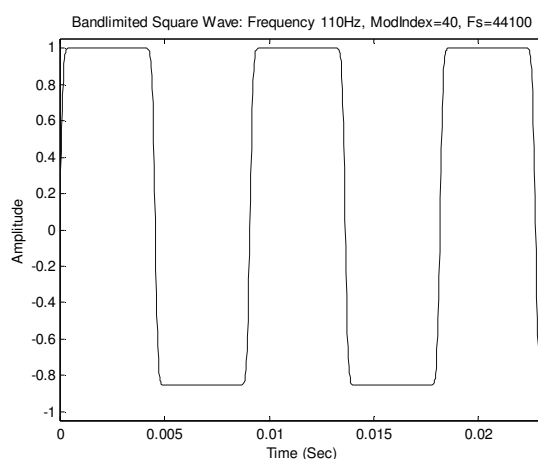


Figure 11: *Bandlimited Square wave produced by integrating the Bipolar Bandlimited Pulse waveform shown in Figure 10.*

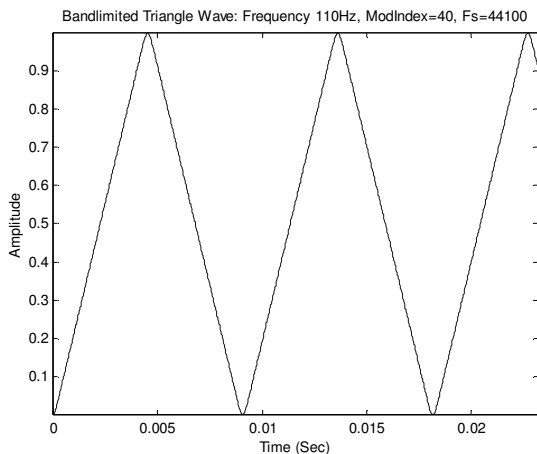


Figure 12: Bandlimited Triangle wave produced by integrating the Bandlimited Square waveform shown in Figure 11.

When generating the square wave mean removal is not an issue but it is important for the triangle waveform. Again, a DC blocking filter [7] is applied to the output of the integrator.

## 5. ASSESSING THE BANDLIMITED SAWTOOTH WAVEFORM

Two experiments were devised to test the quality of this FM synthesis-based Bandlimited sawtooth against a selection of the other approaches. The others included in this test were the Bandlimited Impulse Train (BLIT) of [2], the Bandlimited Step (BLEP) [3], and the Differentiated Parabolic Waveform (DPW) [8]. The modulation index of the FM synthesis-based Bandlimited sawtooth was 98% of the maximum allowable modulation index presented in Figure 7. The BLIT algorithm implemented used the cosine correction suggested by Scavone when the denominator is close to zero [9]. The DPW algorithm was implemented as per [10]. The BLEP algorithm chosen was the version published in [11]. This uses a polynomial functional approximation to bandlimit the sawtooth around the reset points.

### 5.1. Experiment 1

The aim of the first experiment was to measure the proportion of non-harmonic energy in sawtooths generated by the various algorithms. The harmonics in each sawtooth signal were removed using a tuned notch filter that was designed according to [12]. Using an all-pass configuration the notches could be accurately tuned to eliminate the signal's harmonics. The transfer function of the filter is

$$H_{notch}(z) = 0.5(1 - A(z)) \quad (7)$$

where

$$A(z) = \frac{z^{-N} D(z^{-1})}{D(z)} \quad (8)$$

and

$$D(z) = 1 + a_1 z^{-1} + a_2 z^{-2} + \dots + a_N z^{-N} \quad (9)$$

is the all-pass filter denominator coefficients with  $N$  being the filter order. This filter was designed as a Thiran all-pass filter using the Matlab Fractional Delay Filter Toolbox [13].

Denoting  $s(t)$  as the sawtooth signal output from any of the algorithms and  $e(t)$  as the non-harmonic component it contains, the proportion of non-harmonic energy ( $NHE$ ) was computed by

$$NHE = \frac{10 \log_{10} \left( \sum e^2(t) \right)}{10 \log_{10} \left( \sum s^2(t) \right)} \quad (10)$$

To ensure that a sawtooth's harmonics were strongly filtered, two passes of the tuned notch filter were used. Additionally, the summation in Equation (10) ignored the first 0.1 seconds of the signal to avoid including transient energy introduced by the filtering into  $e(t)$ . In this experiment all signals were generated at a sampling frequency of 48000 Hz. The sawtooths were generated at frequencies given by the midi note values 60 to 99. Figure 13 gives the results of this experiment. From the graph it appears that in general the Modified FM-based Bandlimited sawtooth has the least portion of non-harmonic energy present. This can be expected as the modulation index is constrained to keep aliasing low. The performance of the Modified FM-based bandlimited sawtooth improves with increasing note frequency. For the other algorithms the non-harmonic energy level is more consistent over frequency, with the BLEP approach showing the worst performance at low frequencies but the best at high frequencies. The plot for the DPW algorithm appears steady while that of the BLIT oscillates with frequency.

While the result of this experiment is positive for the Modified FM-based Bandlimited sawtooth, its one drawback is that it does not demonstrate how good it matches the ideal digital sawtooth perceptually. The second experiment employed the Perceptual Evaluation of Audio Quality algorithm to test how well each of the sawtooths produced by the different algorithms matched the ideal digital sawtooth.

### 5.2. PEAQ Algorithm

This is the most sophisticated of the psycho-acoustically based audio quality measurement algorithms [14]. It became the ITU standard in 1998. Its basic operation sequence is that it takes a reference and a corrupted signal [15]. These are split into frames. The power spectrum of each frame is computed and then weighted by the frequency response of the outer and middle ear derived from a model. The power spectral energies are then grouped into Critical bands, spaced at 0.25 Bark. An offset is then added to the Critical band energies to compensate for internal noise generated in the ear. A triangular (in dB) spreading function is used to implement spreading in the frequency domain. The excitation function is converted to a loudness representation using Zwicker's model. A neural network system is then used to compare the frames from both signals under a number of different criteria from which a figure of merit indicating the difference between the two is found.

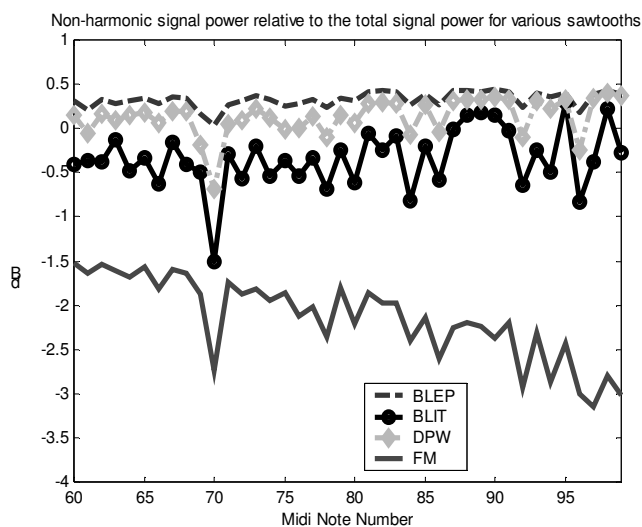


Figure 13: Proportion of Non-Harmonic Signal Energy to Total Signal Power for various sawtooth generating algorithms.

The final measure of sound quality is the Objective Difference Grade which ranges from 0 to -4, where 0 corresponds to imperceptible and -4 is judged as “very annoying”. It has already been successfully applied before in a sound synthesis quality evaluation scenario [16].

### 5.3. Experiment 2

A matlab implementation of the PEAQ algorithm was available from [17]. The reference signal used was an ideal digital sawtooth. Sawtooths for each algorithm were generated at frequencies given by the midi notes from 60 to 99. The sampling frequency was 48000 Hz as this is the one specified by the PEAQ implementation. Figure 14 shows the PEAQ assessment

of the various algorithms. According to the graph, the best overall results are obtained for the Modified FM-based bandlimited sawtooth, while the worst overall is for the BLEP approach. The results for the Modified FM-based bandlimited sawtooth diminish with frequency. The BLIT algorithm has a steady score across the midi-note range, increasing just slightly at midi-note 99. The DPW algorithm performs well at frequencies below 2000 Hz but dips just beyond that point. Interestingly there appears to be some oscillatory behavior in the PEAQ values for the DPW. The BLEP algorithm has a steady performance up to 700Hz but falls after that until steadying out again at 1200Hz.

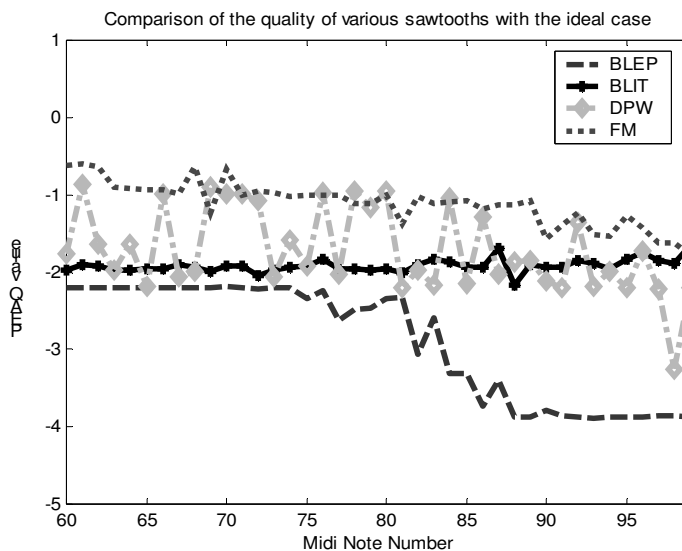


Figure 14: PEAQ results for various algorithms using an Ideal Digital Sawtooth as reference.

## 6. CONCLUSION AND FUTURE WORK

This paper has presented a technique based on Modified FM synthesis for the generation of Bandlimited impulse trains that can be used to produce bandlimited waveforms for subtractive synthesis applications. It has investigated the relationship between the modulation index and aliasing, and also has examined how the Modified FM-based bandlimited sawtooth deviates from an ideal digital sawtooth. Results were then presented to compare its quality with those produced by alternative techniques and they suggest that this method can perform well.

Future work will examine how to modify Equation (1) to increase the magnitudes of the high frequency harmonics particularly at low fundamental frequencies. Another avenue is to reduce the computational complexity of Equation (1) by determining an accurate and fast approximation to the computation of the exponential term. One possibility to investigate is to use a table lookup approach [18].

## 7. REFERENCES

- [1] V. Välimäki and A. Huovilainen, "Antialiasing oscillators in subtractive synthesis," *IEEE Signal Processing Magazine*, vol. 24, no. 2, pp. 116–125, March 2007.
- [2] T. Stilson and J. Smith, "Alias-free digital synthesis of classic analog waveforms," in *Proc. Int. Computer Music Conf.*, Hong Kong, China, pp. 332–335, 1996.
- [3] E. Brandt, "Hard sync without aliasing," in *Proc. Int. Computer Music Conf.*, Havana, Cuba, pp. 365–368, 2001.
- [4] J. Pekonen, "Computationally Efficient Music Synthesis - Methods and Sound Design," Master's thesis, *Helsinki University of Technology*, Helsinki, Finland, 2007.
- [5] J.A. Moorer, "Signal Processing Aspects of Computer Music: A Survey", *Proceedings of the IEEE*, Volume 65, Number 8, August 1977, pp1108-1137.
- [6] J. Chowning, and D. Bristow, *FM Theory & Applications - By musicians for musicians*, Yamaha, Tokyo, 1986.
- [7] R. Yates and R. Lyons, 'DSP Tips & Tricks [DC Blocker Algorithms]', *IEEE Signal Processing Magazine*, vol. 25, no. 2, pp. 132 – 134, March 2008.
- [8] V. Välimäki, "Discrete-time synthesis of the sawtooth waveform with reduced aliasing," *IEEE Signal Processing Lett.*, vol. 12, no. 3, pp. 214–217, Mar. 2005.
- [9] G. Scavone, *Online Lecture Notes*, McGill University, Montreal, Canada, <http://www.music.mcgill.ca/~gary/307/week5/bandlimited.htm>  
URL Checked: 15/5/2008
- [10] V. Välimäki and A. Huovilainen, "Oscillator and Filter Algorithms for Virtual Analog Synthesis", *Computer Music Journal*, vol. 30, no. 2, 2006.
- [11] B. Frei, 'Digital\_Sound\_Generation – Part 1 Oscillators', *Online Book, Institute for Computer Music and Sound Technology*, Zurich University of the Arts, Switzerland.. 2007.  
<http://www.icst.net/dsgdownload/>  
URL Checked: 15/5/2008
- [12] V. Välimäki, M. Ilmoniemi, and M. Huutilainen, "Decomposition and Modification of Musical Instrument Sounds Using a Fractional Delay Allpass Filter," in *Proceedings of the 6th Nordic Signal Processing Symposium (NORSIG 2004)*, Espoo, Finland, June 9-11, 2004.
- [13] T. I. Laakso, V. Välimäki, M. Karjalainen, and U. Laine, "Splitting the unit delay—Tools for fractional delay filter design," *IEEE Signal Processing Magazine*, vol. 13, no. 1, pp. 30–60, Jan. 1996.  
<http://www.acoustics.hut.fi/software/fdtools/>  
URL Checked: 15/5/2008
- [14] ITU-R BS.1387, "Method For Objective Measurement of Perceived Audio Quality", 1998.
- [15] T. Thiede, *Perceptual Audio Quality Assessment using a Non-Linear Filter Bank*, Ph.D. thesis, *Technische Universität Berlin*, Berlin, Germany, 1999.
- [16] B. Hamadicharef and E.C. Ifeachor, "Objective Prediction of Sound Synthesis Quality", *115th AES Convention*, New York, NY, USA, October 10-13, 2003.
- [17] P. Kabal, 'An Examination and Interpretation of ITU-R BS.1387: Perceptual Evaluation of Audio Quality', *TSP Lab Technical Report*, Dept. Electrical & Computer Engineering, McGill University, May 2002.  
[www.mp3-tech.org/programmer/docs/kabalr2002.pdf](http://www.mp3-tech.org/programmer/docs/kabalr2002.pdf)  
URL Checked: 15/5/2008
- [18] F. R. Moore, *Elements of Computer Music*, Prentice Hall, NJ, USA, 1990.